Eur. Phys. J. B **35**, 93–101 (2003)
DOI: 10.1140/epjb/e2003-00259-3

THE EUROPEAN PHYSICAL JOURNAL B

Dynamical exchange effects in the dielectric function of the two-dimensional electron gas

K.J. Hameeuw, F. Brosens, and J.T. Devreese[a]

TFVS, Departement Natuurkunde, Universiteit Antwerpen-UIA, Universiteitsplein 1, 2610 Antwerpen, Wilrijk, Belgium

Received 7 May 2003
Published online 22 September 2003 –

Abstract. Dynamical exchange interactions can be introduced in the dielectric function *via* a dynamic local field factor. We study the effects of this inclusion on both the static and the frequency dependent dielectric function of a two-dimensional electron gas, using the dynamic local field factor that we derived recently *via* the dynamical exchange decoupling method. The results are compared with the dielectric function in the Random Phase Approximation and with different dynamic and static approximations of the local field factor.

PACS. 71.45.Gm Exchange, correlation, dielectric and magnetic response functions, plasmons – 77.22.Ch Permittivity (dielectric function) – 77.55.+f Dielectric thin films

1 Introduction

During the last decades, the two-dimensional (2D) electron gas has remained a fascinating system to study, because in various aspects it behaves quite differently than its three-dimensional (3D) counterpart.

Already in the seventies, Jonson [1] showed that in a 2D electron gas, correlations are much more important than in the 3D case. The Random Phase Approximation (RPA) as well as a Hubbard-like approach [2] showed to be less satisfactory to describe the response of a 2D electron gas to an external field. Therefore, Jonson introduced the correlation effects *via* a static local field factor $\mathcal{G}(q)$ in an STLS-like approach. Several other attempts have been made to describe the correlation effects *via* a static local field factor, more recently by Davoudi *et al.* [4] and Dharma-wardana *et al.* [5]. However, causality arguments [6] and internal consistency requirements in the theory of the electron gas [7] imply the need for a frequency dependent local field factor $\mathcal{G}(q,\omega)$.

Also for the frequency dependent local field factor $\mathcal{G}(q,\omega)$, some attempts have been made to take the correlation effects into account to some extent [8–10]. In the present paper we propose a different approach, based on a variational solution of the time-dependent Hartree-Fock (TDHF) equation for the density matrix, similarly as introduced earlier in three dimensions [11,12]. This approach takes into account the full wave vector and frequency dependence of the exchange correction and has been shown to extend the perturbational calculation of $\mathcal{G}(\mathbf{q},\omega)$ by Czachor *et al.* [8] into a variational description [13]. Furthermore, it is not restricted to imaginary frequencies as in the case of Schulze *et al.* [10].

In three dimensions, Brosens *et al.* [11,12] applied the Hartree-Fock decoupling in the equation of motion for the density matrix of an inhomogeneous electron gas in interaction with an external field. This dynamical exchange decoupling of the four field operator terms in the equation of motion leads to the time-dependent Hartree-Fock (TDHF) equation for the Wigner distribution function, which dynamically includes the exchange contribution. After linearization of the TDHF equation in the external field, the resulting inhomogeneous linear integral equation was solved variationally [14]. *Via* this TDHF approach, the authors obtained an expression for the dynamic local field factor $\mathcal{G}(q,\omega)$ as a sixfold integral, which they reduced analytically to a double integral.

Besides taking into account the full frequency and wave vector dependence of the exchange correction, the TDHF approach has several interesting characteristics.

Firstly, the dynamic local field factor $\mathcal{G}(q,\omega)$ obtained this way is a universal function of the density when expressed in the dimensionless Fermi units $\mathbf{k} = \mathbf{q}/k_F$ and $\nu = \hbar\omega/2E_F$, where k_F and E_F are the Fermi wave vector and the Fermi energy, respectively. Secondly, it obeys the continuity equation for the charge density and several sum rules, as well as the Niklasson relation [15] and the Kimball-Niklasson relation [7,15] for the pair correlation function in the origin $g(0)$, which impose severe restrictions on the frequency dependence of $\mathcal{G}(q,\omega)$. Any static approximation to $\mathcal{G}(q,\omega)$ violates at least one of them, showing that the frequency dependence of $\mathcal{G}(q,\omega)$ has to be included explicitly. The fact that this internal consistency requirements are fulfilled, gives confidence in the

[a] e-mail: devreese@uia.ua.ac.be, jtd@uia.ua.ac.be

variational procedure used to solve the equation of motion for the Wigner distribution function. Last but not least, different energy-loss experiments showed that the TDHF approach considerably improves the agreement with experimental data. This was illustrated in reference [12] for the plasmon frequency and the peak position of the dynamic structure factor $S(q,\omega)$ for aluminum, using experimental data of Batson *et al.* [16], as well as in recent measurements of the dynamic local field factor in aluminum by Larson *et al.* [17,18].

Because of these interesting features of the dynamical exchange decoupling method, it seems natural to extend this approach to study the dynamic exchange effects in a two-dimensional (2D) electron gas. Given the present lack of experiments that can clearly distinguish the effects of the exchange corrections in two dimensions, the results will rather have a predictive value.

2 Dynamical exchange decoupling in two dimensions

Applying the TDHF approach to a 2D electron gas requires some rather straightforward adaptations to the equation of motion, leading to a dielectric function

$$\epsilon(q,\omega) = 1 + \frac{Q_0(q,\omega)}{1 - \mathcal{G}(q,\omega)\, Q_0(q,\omega)}. \tag{1}$$

In two dimensions, $\mathcal{G}(q,\omega)$ can be expressed as a fourfold integral. The function $Q_0(q,\omega)$ is the 2D analogon of the Lindhard polarizability and is known in closed form [19].

As mentioned earlier and deduced in reference [13], the local field factor obtained *via* the variational approach exhibits a scaling property with respect to the density. If the wave vector and the frequency are expressed in Fermi units ($\mathbf{k} = \mathbf{q}/k_F, \nu = \hbar\omega/2E_F$), the dynamic local field factor as obtained in expression (1) is a universal function of $\mathbf{k}$ and ν for all densities. In these units, its explicit expression is given by

$$G(k,\nu) = \mathcal{G}(kk_F, 2\nu E_F/\hbar) = \lim_{\delta\to 0} \frac{r_s^2}{4k\pi^2} \frac{I_G(k,\nu)}{Q_0^2\left(kk_F, \frac{2\nu E_F}{\hbar}\right)}. \tag{2}$$

The function $Q_0\left(kk_F, \frac{2\nu E_F}{\hbar}\right)$ is linear in the Wigner-Seitz radius r_s and the function $I_G(k,\nu)$ is a fourfold integral with respect to the variables $\mathbf{r}$ and $\mathbf{r}'$,

$$I_G(k,\nu) = \int d^2r \int d^2r' \times \frac{\left(\mathcal{N}\left(\mathbf{r}+\frac{\mathbf{k}}{2}\right) - \mathcal{N}\left(\mathbf{r}-\frac{\mathbf{k}}{2}\right)\right)\left(\mathcal{N}\left(\mathbf{r}'+\frac{\mathbf{k}}{2}\right) - \mathcal{N}\left(\mathbf{r}'-\frac{\mathbf{k}}{2}\right)\right)}{|\mathbf{r}-\mathbf{r}'|} \times \frac{1}{\nu + i\delta - \mathbf{r}\cdot\mathbf{k}} \left(\frac{1}{\nu + i\delta - \mathbf{r}'\cdot\mathbf{k}} - \frac{1}{\nu + i\delta - \mathbf{r}\cdot\mathbf{k}}\right), \tag{3}$$

with

$$\mathcal{N}(\mathbf{r}) = \begin{cases} 1 & \text{if } |\mathbf{r}| \le 1, \\ 0 & \text{if } |\mathbf{r}| > 1. \end{cases} \tag{4}$$

This density independence of the local field factor $G(k,\nu)$ makes it worthwhile to tabulate $G(k,\nu)$ for different values of k and ν.

In reference [8], Czachor *et al.* obtained the same type of integral (3) when calculating the first order self-energy and exchange contributions to the proper polarizability $Q(q,\omega)$. Their perturbative approach leads to a dielectric function

$$\epsilon^{(1)}(q,\omega) = 1 + Q_0(q,\omega) + Q_1(q,\omega). \tag{5}$$

It turns out that the function $Q_1(q,\omega)$ is given by $Q_1(q,\omega) = r_s^2 I_G(k,\nu)/4\pi^2 k$. Writing expression (5) in the standard form

$$\epsilon^{(1)}(q,\omega) = 1 + \frac{Q_0(q,\omega)}{1 - \mathcal{G}^{(1)}(q,\omega)\, Q_0(q,\omega)}, \tag{6}$$

leads to

$$\epsilon^{(1)}(q,\omega) = 1 + Q_0(q,\omega)\left(1 + \mathcal{G}(q,\omega)\, Q_0(q,\omega)\right). \tag{7}$$

Thus the dielectric function $\epsilon^{(1)}(q,\omega)$ obtained by Czachor *et al.* is the first order term in the perturbation expansion of the variational $\epsilon(q,\omega)$ if $\mathcal{G}(q,\omega)$ is assumed to be small. It is clear from expressions (5) and (6) that $\mathcal{G}^{(1)}(q,\omega)$, when expressed in Fermi units, cannot be density independent.

In Appendix A we present an alternative calculation as compared to Czachor *et al.* to reduce the fourfold integral $I_G(k,\nu)$ analytically into a double integral. Because the different contributions to the integrand are treated on the same footing, this alternative procedure is numerically more stable and more accurate than the method proposed in reference [8].

3 The dielectric function

The dielectric function $\varepsilon(k,\nu) = \epsilon(kk_F, 2\nu E_F/\hbar)$ only depends on the density *via* the linear r_s dependence of the Lindhard polarizability $Q_0\left(kk_F, \frac{2\nu E_F}{\hbar}\right)$. We discuss the static and the frequency dependent dielectric function in more detail.

3.1 Static dielectric function $\varepsilon(\mathbf{k}, 0)$

In the static limit, the imaginary part of $G(k,0)$ vanishes and one is left with

$$G(k,0) = \lim_{\delta\to 0} \frac{r_s^2}{4k\pi^2} \frac{1}{Q_0^2(kk_F,0)} \times \int d^2r \int d^2r' \frac{(\mathbf{r}-\mathbf{r}')\cdot\mathbf{k}}{(\mathbf{r}\cdot\mathbf{k})^2 (\mathbf{r}'\cdot\mathbf{k})} \times \frac{\left(\mathcal{N}\left(\mathbf{r}+\frac{\mathbf{k}}{2}\right) - \mathcal{N}\left(\mathbf{r}-\frac{\mathbf{k}}{2}\right)\right)\left(\mathcal{N}\left(\mathbf{r}'+\frac{\mathbf{k}}{2}\right) - \mathcal{N}\left(\mathbf{r}'-\frac{\mathbf{k}}{2}\right)\right)}{|\mathbf{r}-\mathbf{r}'|}. \tag{8}$$

We opted for a straightforward numerical calculation of $G(k,0)$, following the same procedure as for the dynamic

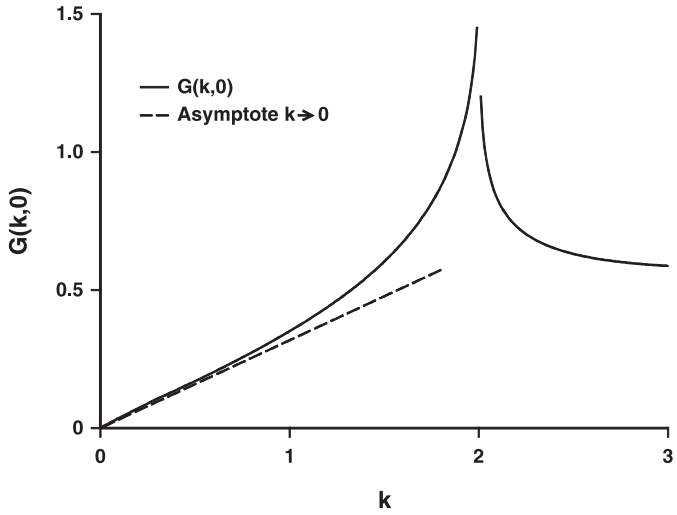

Fig. 1. The static local field factor $G(k,0)$ for $r_s = 1.5$. The dashed line shows the asymptotic behaviour of $G(k,0)$ for $k \to 0$.

local field factor, with the frequency put equal to zero. Only when k tends to zero, the accuracy of this straightforward calculation is less satisfactory, yet the asymptotic behavior of $G(k,0)$ for $k \to 0$ is easily obtained analytically

$$\lim_{k\to 0} G(k,0) = \frac{k}{\pi}. \tag{9}$$

The function $G(k,0)$ is plotted in Figure 1, together with its asymptotic behavior in the long-wavelength limit. Similarly as in 3D, the function $G(k,0)$ shows a spike at $k = 2$. This peak is due to the fact that at $k = 2$, the singular behavior of $G(k,\nu)$ at the boundaries of the Landau continuum is suppressed, leaving a steep but finite spike in the real part of $G(k,\nu)$ for $\nu \to 0$. Due to numerical inaccuracy in the region around the spike, its height is not exactly known. In 3D, the physical relevance of the occurrence of such a peak has been illustrated in the calculation of the screening of the electron-ion potential in metals [20]. Recently, Dharma-wardana *et al.* [5] calculated the static 2D local field factor using a mapping of the 2D quantum fluid to a classical Coulomb fluid [21]. Their local field factor shows a maximum near $k = 3$. The position of the peak at $k = 2$ in the TDHF approach however, is determined by the boundaries of the Landau continuum. As already discussed in reference [13], the 2D Lindhard distribution function $Q_0(q,\omega)$ fixes the boundaries of the pair creation and annihilation region by taking into account the free-particle energy spectrum only, neglecting the exchange interactions. Another choice of distribution function which does take into account the exchange interactions in the one-particle spectrum could change the position of the boundaries and thus of the peak position in the static local field factor.

For $k \to \infty$, the asymptotic behavior of $G(k,0)$ can again be calculated analytically. It is easily shown that

$$\lim_{k\to\infty} G(k,0) = \frac{1}{2}. \tag{10}$$

Since only exchange effects are included in the local field factor, no linear term due to correlation effects occurs, as found by Davoudi *et al.* [4]. The expressions (9) and (10) agree with the results found by Iwamoto [22]. The long- and short-wavelength limits of the static local field factor provide an adequate way to check the consistency of the approximations made in deriving $\varepsilon(k,\nu)$ in the TDHF approach.

In the static case, an important consistency requirement is provided by the compressibility sum rule, which relates the long-wavelength limit of the static dielectric function with the compressibility of the electron gas. In 2D, one finds

$$\lim_{q\to 0} \epsilon(q,0) = 1 + \frac{k_{TF}}{q}\frac{\kappa^T}{\kappa_0^T}, \tag{11}$$

where κ^T is the isotherm compressibility and k_{TF} the Thomas-Fermi wave vector. The asymptotic behavior of $\varepsilon(k,0)$ in the long-wavelength limit follows immediately from (9) and (1)

$$\lim_{k\to 0} \varepsilon(k,0) = 1 + r_s\sqrt{2}\frac{1}{k}\frac{1}{1-\frac{\sqrt{2}r_s}{\pi}}. \tag{12}$$

This result agrees with the compressibility sum rule of the 2D electron gas from the Hartree-Fock ground state energy in (11). Such agreement with the Hartree-Fock approximation is to be expected, because in the static case, the dynamical exchange decoupling reduces to the Hartree-Fock approximation. As in the 3D case, it shows that the assumptions made when variationally solving the TDHF equations do not break down the internal consistency of the dynamical exchange decoupling method [12]. The long-wavelength limit of the static dielectric function in the perturbative approach [8] is

$$\lim_{k\to 0} \varepsilon^{(1)}(k,0) = 1 + \frac{1}{k}\sqrt{2}r_s\left(1 + \frac{\sqrt{2}r_s}{\pi}\right), \tag{13}$$

which fails to fulfil the compressibility sum rule in the Hartree-Fock approximation.

In the long-wavelength limit, the static dielectric function diverges for $r_s = \pi/\sqrt{2} = 2.2214$. This implies an instability of the electron gas in the Hartree-Fock approximation for $r_s \geq 2.2214$, as the compressibility modus changes sign. Furthermore, a Bloch-type instability of the paramagnetic Hartree-Fock ground state occurs at $r_s = 2.0111$, pointing to the possibility of the formation of spin-density waves. Therefore, one could argue that the dynamical exchange decoupling approach, combined with a paramagnetic ground state, becomes questionable for $r_s \geq 2$, where a region of negative $\varepsilon(k,0)$ appears, although Rajagopal *et al.* have shown that the region of paramagnetic stability could extend up to $r_s \leq 2.3$ if one includes higher order exchange diagrams. In Figure 2, $\varepsilon(k,0)$ in the TDHF approach is shown in comparison with the static dielectric function in the RPA approach and $\varepsilon^{(1)}(k,0)$ in the perturbative approach for $r_s = 1.5$.

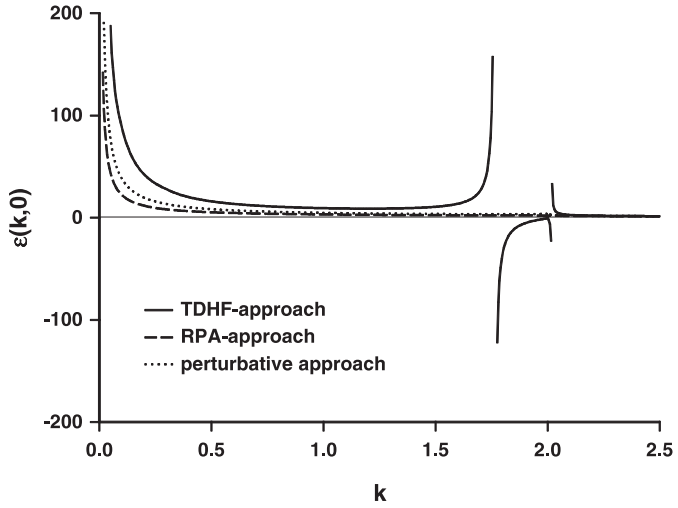

Fig. 2. The static dielectric function $\varepsilon(k,0)$ in the TDHF-approach (full curve) for $r_s = 1.5$, compared to the static dielectric function $\varepsilon^{RPA}(k,0)$ in the RPA-approach (dashed curve) and $\varepsilon^{(1)}(k,0)$ in the perturbative approach (dotted curve).

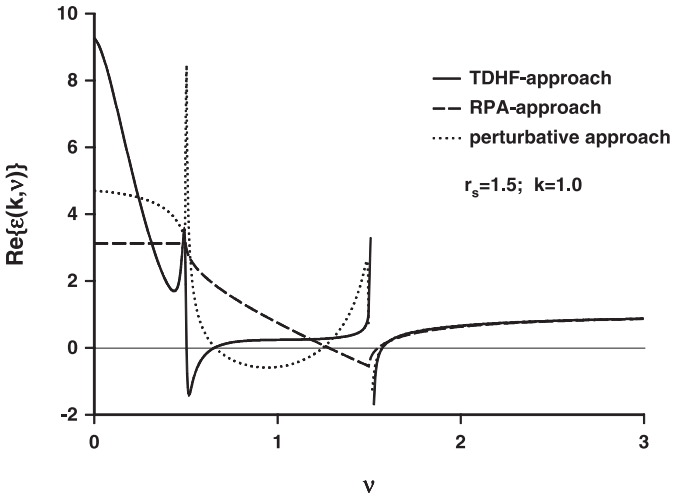

Fig. 3. The real part of the frequency dependent dielectric function $\varepsilon(k,\nu)$ in the TDHF-approach (full curve) for $r_s = 1.5$ and $k = 1$, compared to the real part of the dielectric function $\varepsilon^{RPA}(k,\nu)$ in the RPA-approach (dashed curve) and of the dielectric function $\varepsilon^{(1)}(k,\nu)$ in the perturbative approach (dotted curve).

Since the static local field factor exceeds 1 around $k = 2$, it is clear from expression (1) that a pole can occur in the static dielectric function for certain values of r_s. For $r_s = 1.5$, even two poles exist around $k = 1.763$ and $k = 2.016$.

3.2 Frequency dependent dielectric function $\varepsilon(\mathbf{k},\nu)$

In Figure 3 (Figure 4) we show the real (imaginary) part of the dielectric function $\varepsilon(k,\nu)$ for $r_s = 1.5$ and $k = 1$. Again the dielectric functions in the TDHF approach, the perturbative approach and the RPA approach are shown. The real part $\mathrm{Re}\{\varepsilon(k,\nu)\}$ in the TDHF approach varies strongly. Approaching $\nu = k + k^2/2$ from the right, $\mathrm{Re}\{\varepsilon(k,\nu)\}$ has a pole of first order before it reaches the value $\mathrm{Re}\{\varepsilon(k,\nu)\} = 1$ at $\nu = k + k^2/2$. At the boundary $\nu = |k - k^2/2|$ similar behavior occurs. However, the function $\mathrm{Re}\{\varepsilon(k,\nu)\}$ has no first order pole here because of the existence of an imaginary part of $G(k,\nu)$ and $Q_0(k,\nu)$ for $\max\{0, k^2/2 - k\} \leq \nu \leq k + k^2/2$. The real part $\mathrm{Re}\{\varepsilon^{RPA}(k,\nu)\}$ in the RPA approach remains constant up to $\nu = |k - k^2/2|$, decreases to a minimum at $\nu = k + k^2/2$ and then slowly rises to its asymptotic value $\mathrm{Re}\{\varepsilon^{RPA}(k,\nu)\} = 1$ at infinity. In the perturbative approach, the real part of $\mathrm{Re}\{\varepsilon^{(1)}(k,\nu)\}$ diverges both at $\nu = k + k^2/2$ and $\nu = |k - k^2/2|$.

For $\nu \gg k + k^2/2$, $\mathrm{Re}\{\varepsilon^{RPA}(k,\nu)\}$ and $\mathrm{Re}\{\varepsilon(k,\nu)\}$ almost coincide. This would mean that no strong influence of the exchange effects will be seen in the plasmon dispersion, as can be expected because of the collective nature of the plasmon excitation. The long-wavelength limit of $\mathrm{Re}\{G(k,\nu > k^2/2 + k)\}$ can again be calculated analytically. The imaginary part $\mathrm{Im}\{G(k,\nu > k^2/2 + k)\}$ is zero in this region. For the details of the calculation, we

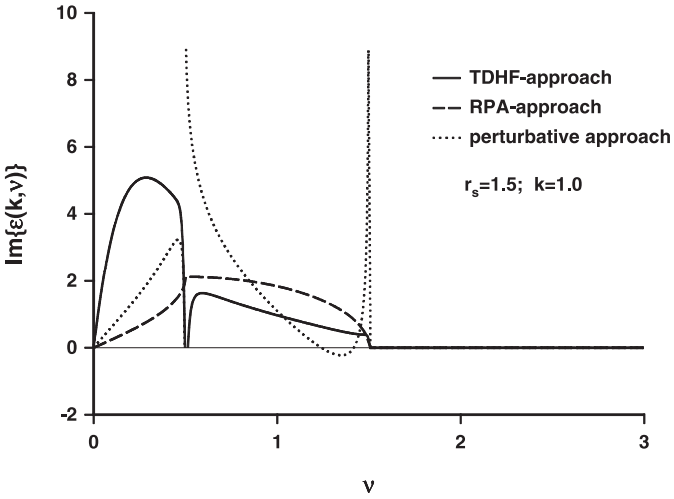

Fig. 4. The imaginary part of the frequency dependent dielectric function $\varepsilon(k,\nu)$ in the TDHF-approach (full curve) for $r_s = 1.5$ and $k = 1$, compared to the imaginary part of the dielectric function $\varepsilon^{RPA}(k,\nu)$ in the RPA-approach (dashed curve) and of the dielectric function $\varepsilon^{(1)}(k,\nu)$ in the perturbative approach (dotted curve).

refer to Appendix B. To lowest order in k, one finds

$$\lim_{k\to 0,\nu>k^2/2+k} \mathrm{Re}\{G(k,\nu)\} = \frac{5}{6\pi}k.$$

The long wavelength limit of the dielectric function in the TDHF approach to order k^3 is

$$\lim_{k\to 0,\nu>k^2/2+k} \varepsilon(k,\nu) = 1 - \frac{r_s}{\sqrt{2}\nu^2}k\frac{1+\frac{3}{4}\frac{k^2}{\nu^2}}{1+\frac{5\sqrt{2}r_s}{12\pi\left(1+\frac{3}{4}\frac{k^2}{\nu^2}\right)}\frac{k^2}{\nu^2}}. \quad (14)$$

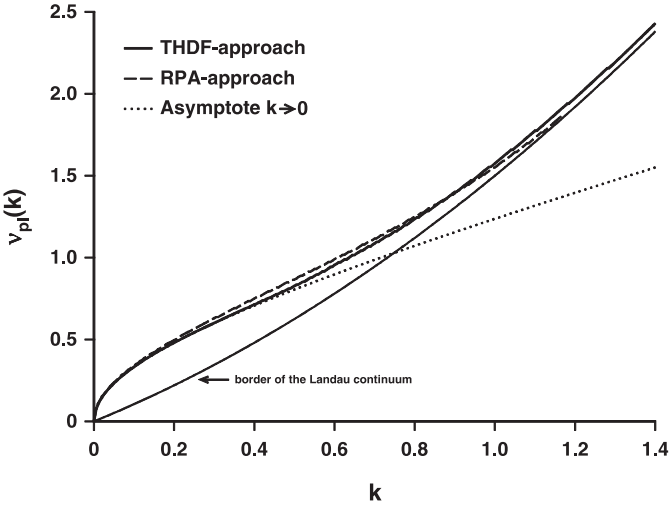

Fig. 5. The plasmon branch in the TDHF-approach (full curve) and the RPA-approach (dashed curve) for $r_s = 1.5$ and $k = 1$. The asymptotic behaviour for $\nu_{pl}(k)$ in the TDHF-approach as $k \to 0$ is also shown (dotted curve).

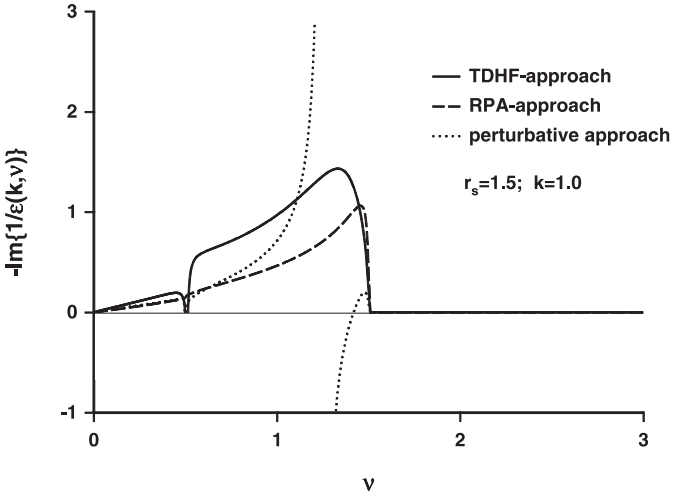

Fig. 6. The energy-loss function $-\operatorname{Im}\{1/\varepsilon(k,\nu)\}$ in the TDHF-approach (full curve) for $r_s = 1.5$ and $k = 1$, compared to the energy-loss function $-\operatorname{Im}\left\{1/\varepsilon^{RPA}(k,\nu)\right\}$ in the RPA-approach (dashed curve) and $-\operatorname{Im}\left\{1/\varepsilon^{(1)}(k,\nu)\right\}$ in the perturbative approach (dotted curve).

The plasmon frequency in the long-wavelength limit is thus found to be

$$\lim_{k\to 0,\nu>k^2/2+k} \nu_{pl}^2(k) \cong \frac{r_s k}{\sqrt{2}}\left(1+\frac{3\sqrt{2}}{4r_s}\left(1-\frac{5\sqrt{2}}{9\pi}r_s\right)k\right), \tag{15}$$

where the third term on the right hand side is the correction term to the RPA. This gives indeed only a small attenuation of the plasmon as compared to RPA as k tends to zero. The plasmon branches in the TDHF approach and the RPA approach are shown in Figure 5 for $r_s = 1.5$.

The imaginary part $\operatorname{Im}\left\{\varepsilon^{RPA}(k,\nu)\right\}$ in the RPA approach starts at zero, rises to its maximum value at $\nu = \left|k - k^2/2\right|$ and decreases back to zero at $\nu = k + k^2/2$. The imaginary part $\operatorname{Im}\{\varepsilon(k,\nu)\}$ in the TDHF approach has a more pronounced structure. Given the behavior of the functions $\operatorname{Re}\{G(k,\nu)\}$ and $\operatorname{Im}\{G(k,\nu)\}$, it can be shown analytically that

$$\lim_{\nu\to|k^2/2-k|} \operatorname{Im}\{\varepsilon(k,\nu)\} = 0,$$

although this correct limit can hardly be obtained numerically. Therefor, a small region around the boundary $\nu = \left|k - k^2/2\right|$ is left out of the graph.

The imaginary part $\operatorname{Im}\{\varepsilon(k,\nu)\}$ in the TDHF approach thus fulfils the requirement that $\operatorname{Im}\{\varepsilon(k,\nu)\}$ should be positive. This requirement stems from the fact that the imaginary part of the inverse dielectric function $\epsilon^{-1}(q,\omega)$ is proportional to the structure factor $S(q,\omega)$, which gives the probability density to create an excitation with given wave number q and frequency ω of the electron gas

$$S(q,\omega) \propto -\operatorname{Im}\left\{\frac{1}{\epsilon(q,\omega)}\right\}.$$

In a consistent theory of the dielectric response, the structure factor $S(q,\omega)$ should naturally be positive.

As is clear from Figure 4, the imaginary part $\operatorname{Im}\left\{\varepsilon^{(1)}(k,\nu)\right\}$ in the perturbative approach of Czachor *et al.*, becomes negative in a distinctive region of its domain for larger values of r_s. This is an intrinsic property of $\operatorname{Im}\left\{\varepsilon^{(1)}(k,\nu)\right\}$, independent of the behavior of $\mathcal{G}^{(1)}(q,\omega)$ at the boundaries of the Landau continuum. The dielectric function in the perturbative approach thus violates an important consistency requirement, both in 2D and in 3D [24].

Figure 6 shows the energy-loss function $-\operatorname{Im}\{1/\varepsilon(k,\nu)\}$ at $r_s = 1.5$ and $k = 1$, as compared to the energy-loss function in the RPA approach and in the perturbative approach. Again it is clear from the figure that $-\operatorname{Im}\left\{1/\varepsilon^{(1)}(k,\nu)\right\}$ becomes negative in a distinct region of its domain.

4 Conclusions

In the present paper, we studied the linear response of a 2D electron gas, using a novel expression for the frequency dependent local field factor $\mathcal{G}(q,\omega)$ which we deduced earlier [13]. The inclusion of these dynamical exchange effects has a pronounced influence on the dielectric function. Both the static and the frequency dependent dielectric function have been studied. The internal consistency of the TDHF approach in three dimensions has been shown to apply also for the 2D case, a feature that is not reproduced by *e.g.* the perturbative approach of reference [8]. Furthermore, our approach extents this perturbative approach and is not limited to imaginary frequencies as in reference [10]. Awaiting experimental data, only theoretical results have been given for the energy-loss function. Direct measurements of the local field factor as reported recently by Tischer *et al.* [18] in the 3D case, are not yet available in two dimensions.

$$I_G(k,\nu) = \sum_{\ell,\ell'=\pm 1} \ell\ell' \int_{-\infty}^{\infty}\int_{-\infty}^{\infty}\int_{-\infty}^{\infty}\int_{-\infty}^{\infty} \frac{1}{\nu+i\delta-xk}\left(\frac{1}{\nu+i\delta-x'k}-\frac{1}{\nu+i\delta-xk}\right) \times \frac{\Theta\left(\left(x+\frac{\ell}{2}k\right)^2+y^2\le 1\right)\Theta\left(\left(x'+\frac{\ell'}{2}k\right)^2+(y')^2\le 1\right)}{\sqrt{(x-x')^2+(y-y')^2}} dxdydx'dy'. \quad (A.1)$$

$$Y(a,b,s) = \int_{-\infty}^{\infty}\int_{-\infty}^{\infty} \frac{\Theta\left(a^2+y^2\le 1\right)\Theta\left(b^2+(y')^2\le 1\right)}{\sqrt{s^2+(y-y')^2}} dy'dy. \quad (A.2)$$

$$Y(a,b,s) = 2\Theta\left(a^2\le 1\right)\Theta\left(b^2\le 1\right)\begin{pmatrix} \left(\sqrt{1-a^2}+\sqrt{1-b^2}\right)\operatorname{arcsinh}\frac{\sqrt{1-a^2}+\sqrt{1-b^2}}{|s|} \\ -\left(\sqrt{1-a^2}-\sqrt{1-b^2}\right)\operatorname{arcsinh}\frac{\sqrt{1-a^2}-\sqrt{1-b^2}}{|s|} \\ +\sqrt{s^2+\left(\sqrt{1-a^2}-\sqrt{1-b^2}\right)^2}-\sqrt{s^2+\left(\sqrt{1-a^2}+\sqrt{1-b^2}\right)^2} \end{pmatrix}. \quad (A.3)$$

This work is performed within the framework of the FWO projects No. 1.5.545.98, G.0287.95, G.0071.98, and WO.073.94N [Wetenschappelijke Onderzoeksgemeenschap van het FWO over "Laagdimensionele systemen" (Scientific Research Community on Low-Dimensional Systems)], the "Interuniversitaire Attractiepolen – Belgische Staat, Diensten van de Eerste Minister – Wetenschappelijke, Technische en Culturele Aangelegenheden" (Interuniversity Poles of Attraction Programs –Belgian State, Prime Minister's Office –Federal Office for Scientific, Technical and Cultural Affairs), and in the framework of the GOA BOF UA 2000 projects of the Universiteit Antwerpen. One of the authors (K.J.H.) likes to thank J. Tempere for helpful discussions. K.J.H. (Aspirant bij het Fonds voor Wetenschappelijk Onderzoek -Vlaanderen), also acknowledges the FWO-Vlaanderen for financial support.

Appendix A: The fourfold integral $I_G(k,\nu)$

It is possible to reduce the fourfold integral $I_G(k,\nu)$ (3) analytically into a twofold integral. As compared to reference [8], we present an alternative approach.

Introduce a Cartesian coordinate frame $\mathbf{r}=(x,y)$, $\mathbf{r}'=(x',y')$, where the x axis and the x' axis are chosen in the direction of the wave vector $\mathbf{k}$. The fourfold integral (3) then becomes

see equation (A.1) above

The function $\Theta(\lambda)$, with λ a logical expression, denotes $\Theta(\lambda)=1$ if λ is true, and $\Theta(\lambda)=0$ if λ is false. The integration over the variables y and y' can be done analytically. We introduce the auxiliary function $Y(a,b,s)$, defined as

see equation (A.2) above

This function has the symmetry properties $Y(a,b,s) = Y(b,a,s) = Y(b,a,-s)$. Written in closed form (A.2) yields

see equation (A.3) above

The function is zero at the boundaries of its domain, $Y(\pm 1,b,s) = Y(a,\pm 1,s) = 0$, and displays a logarithmic singularity as $s\to 0$.

Introducing the function $Y(a,b,s)$ in the expression (A.1) and translating the integration variables leads to

$$I_G(k,\nu) = \sum_{\ell,\ell'=\pm 1}\ell\ell'\frac{1}{k^2}\int_{-\infty}^{\infty}\int_{-\infty}^{\infty}\frac{1}{w_\ell+i\delta-r} \times\left(\frac{1}{w_{\ell'}+i\delta-s}-\frac{1}{w_\ell+i\delta-r}\right) \times Y\left(r,s,r-s-(\ell-\ell')\frac{k}{2}\right)drds, \quad (A.4)$$

where we defined the parameter $w_\ell = w_\ell(k,\nu) = \nu/k + \ell k/2$.

The function $I_G(k,\nu)$ then naturally splits into two parts.

$$I_G(k,\nu) = \frac{1}{k^2}\left(I_1(k,\nu) - I_2(k,\nu)\right), \quad (A.5)$$

with

$$I_1(k,\nu) = \sum_{\ell,\ell'=\pm 1}\ell\ell'\frac{1}{k^2}\int_{-\infty}^{\infty}\int_{-\infty}^{\infty}\frac{1}{w_\ell+i\delta-r}\frac{1}{w_{\ell'}+i\delta-s} \times Y\left(r,s,r-s-(\ell-\ell')\frac{k}{2}\right)drds, \quad (A.6a)$$

$$I_2(k,\nu) = \sum_{\ell,\ell'=\pm 1}\ell\ell'\frac{1}{k^2}\int_{-\infty}^{\infty}\int_{-\infty}^{\infty}\frac{1}{(w_\ell+i\delta-r)^2} \times Y\left(r,s,r-s-(\ell-\ell')\frac{k}{2}\right)drds. \quad (A.6b)$$

$$I_G(k,\nu) = \frac{1}{k^2}\sum_{\ell,\ell'=\pm 1}\ell\ell'\int_{-\infty}^{\infty}\int_{-\infty}^{\infty}\frac{\frac{2Y\left(r,s,r-s-\left(\ell-\ell'\right)\frac{k}{2}\right)}{s-r-\left(\ell'-\ell\right)\frac{k}{2}}+X\left(r,s,r-s-\left(\ell-\ell'\right)\frac{k}{2}\right)}{r-w_\ell-i\delta}dsdr. \tag{A.11}$$

$$\mathrm{Im}\left\{I_G(k,\nu)\right\} = \frac{\pi}{k^2}\sum_{\ell=\pm 1}\Theta\left(w_\ell^2(k,\nu)\le 1\right)\int_{-1}^{1}\begin{pmatrix}2\left(\frac{Y(s,w_\ell,s-w_\ell)}{s-w_\ell}-\frac{Y(s,w_\ell,s-(w_\ell-\ell k))}{s-(w_\ell-\ell k)}\right)\\ +X(s,w_\ell,s-w_\ell)-X(s,w_\ell,s-(w_\ell-\ell k))\end{pmatrix}ds, \tag{A.12}$$

$$\mathrm{Re}\left\{I_G(k,\nu)\right\} = \frac{1}{k^2}\sum_{\ell=\pm 1}\mathcal{P}\int_{-1}^{1}\frac{1}{r-w_\ell}\int_{-1}^{1}\begin{pmatrix}2\left(\frac{Y(s,r,s-r)}{s-r}-\frac{Y(s,r,s-(r-\ell k))}{s-(r-\ell k)}\right)\\ +X(s,r,s-r)-X(s,r,s-(r-\ell k))\end{pmatrix}dsdr. \tag{A.13}$$

For the first part $I_1(k,\nu)$, partial fractions allow to decouple the product of first order poles

$$\frac{1}{w_\ell+i\delta-r}\frac{1}{w_{\ell'}+i\delta-s} = \frac{1}{r-s-\left(\ell-\ell'\right)\frac{k}{2}}\left(\frac{1}{w_\ell+i\delta-r}-\frac{1}{w_{\ell'}+i\delta-s}\right). \tag{A.7}$$

Interchanging the integration variables r and s to concentrate the frequency dependence in the integral over r, gives

$$I_1(k,\nu) = 2\sum_{\ell,\ell'=\pm 1}\ell\ell'\int_{-\infty}^{\infty}\frac{1}{w_\ell+i\delta-r}\times\int_{-\infty}^{\infty}\frac{1}{r-s-\left(\ell-\ell'\right)\frac{k}{2}}Y\left(r,s,r-s-\left(\ell-\ell'\right)\frac{k}{2}\right)dsdr. \tag{A.8}$$

The second part $I_2(k,\nu)$ has a second-order pole in the integrand. Because $Y(a,b,s)=0$ at the boundaries of its domain, an integration by parts allows us to reduce this second-order pole into a first-order pole *via*

$$\frac{1}{\left(w_\ell+i\delta-r\right)^2} = \frac{\partial}{\partial r}\frac{1}{w_\ell+i\delta-r}.$$

Performing the subsequent integrations leads to

$$I_2(k,\nu) = \sum_{\ell,\ell'=\pm 1}\ell\ell'\int_{-\infty}^{\infty}\frac{1}{w_\ell+i\delta-r}\times\int_{-\infty}^{\infty}X\left(r,s,r-s-\left(\ell-\ell'\right)\frac{k}{2}\right)dsdr, \tag{A.9}$$

where a new auxiliary function $X(a,b,s)$ is defined as

$$X(a,b,s) = 2\Theta\left(a^2\le 1\right)\Theta\left(b^2\le 1\right)\times\begin{pmatrix}\left(\frac{a}{\sqrt{1-a^2}}+\frac{b}{\sqrt{1-b^2}}\right)\mathrm{arcsinh}\,\frac{\sqrt{1-a^2}+\sqrt{1-b^2}}{|s|}\\ -\left(\frac{a}{\sqrt{1-a^2}}-\frac{b}{\sqrt{1-b^2}}\right)\mathrm{arcsinh}\,\frac{\sqrt{1-a^2}-\sqrt{1-b^2}}{|s|}\end{pmatrix}. \tag{A.10}$$

The function $X(a,b,s)$ also displays a logarithmic singularity as $s\to 0$, but does not vanish at its domain boundaries, $X(\pm 1,b,s)\neq X(a,\pm 1,s)\neq 0$.

Putting the different parts together again, expression (A.4) is transformed into

see equation (A.11) above

The real and imaginary part of $I_G(k,\nu)$ are readily found by making use of the formula of Plemelj $\frac{1}{p+i\varepsilon}=\mathcal{P}\frac{1}{p}-i\pi\delta(p)$, where $\mathcal{P}$ denotes the principal value. Rewriting the summation over ℓ and ℓ' and making use of the symmetry properties of the functions $X(a,b,s)$ and $Y(a,b,s)$ then finally yields

see equation (A.12) and (A.13) above

The functions $\Theta(\lambda)$ that occur in the definitions of $X(a,b,s)$ and $Y(a,b,s)$ have been made explicit in the above expressions.

The imaginary part $\mathrm{Im}\left\{I_G(k,\nu)\right\}$ only differs from zero in distinct regions in the (k,ν)-plane where at least one of the Θ-functions is nonzero. This domain of the (k,ν)-plane is known as the pair creation and annihilation region. At the boundaries of these regions, defined by $w_\ell=\pm 1$, the imaginary part of $I_G(k,\nu)$ displays singular behavior. The function $X(a,b,s)$ displays an inverse square root singularity if $a,b\to 1$. This means that the imaginary part $\mathrm{Im}\left\{I_G(k,\nu)\right\}$ displays an inverse square root singularity as $|w_\ell|\overset{<}{\to}1$. Only one integral remains to be calculated numerically for $\mathrm{Im}\left\{I_G(k,\nu)\right\}$. However, this numerical integration is rather cumbersome because of the singularities in the integrand. Both $X(a,b,s)$ and $Y(a,b,s)$ display a logarithmic singularity as $s\to 0$. Moreover, a pole of first order occurs in the integrand and, as said, the function $X(a,b,s)$ displays an inverse square root singularity if $a,b\to 1$. A stable integration routine has been worked out.

The real part $\mathrm{Re}\left\{I_G(k,\nu)\right\}$ can either be obtained directly from (A.13) or from $\mathrm{Im}\left\{I_G(k,\nu)\right\}$ *via* the Hilbert transform

$$\mathrm{Re}\left\{I_G(k,\nu)\right\} = \frac{1}{\pi}\mathcal{P}\int_{-\infty}^{\infty}\frac{\mathrm{Im}\left\{I_G(k,\nu')\right\}}{\nu'-\nu}d\nu'. \tag{A.14}$$

The inverse square root singularity in $\mathrm{Im}\left\{I_G(k,\nu)\right\}$ substantially hampers an accurate calculation of

$$\lim_{k\to 0,\nu>k^2/2+k} \mathrm{Re}\left\{I_G\left(k,\nu\right)\right\} = \frac{4k^4}{\nu^4}\int_0^\infty\int_0^\infty \frac{\frac{1-t^2}{1+t^2}\frac{1-s^2}{1+s^2}\left(\frac{1-t^2}{1+t^2}+2\frac{1-s^2}{1+s^2}\right)\left(\frac{1-t^2}{1+t^2}-\frac{1-s^2}{1+s^2}\right)}{\sqrt{1+t^2}\sqrt{1+s^2}}\frac{|s+t|+|s-t|}{|s-t|\,|s+t|}\,ds\,dt, \tag{B.9}$$

$\mathrm{Re}\left\{I_G\left(k,\nu\right)\right\}$ and produces the same kind of singularity in the real part of $I_G\left(k,\nu\right)$ for $|w_\ell| \stackrel{>}{\to} 1$.

Appendix B: Limiting behavior of G (k, ν)

For arbitrary k and ν, the function $G\left(k,\nu\right)$ is only known numerically. Nevertheless, exact analytic expressions for $G\left(k,\nu\right)$ can be obtained in several limiting cases. The short- and long-wavelength limit of the static local field factor are obtained almost straightaway from expression (8) as

$$\lim_{k\to 0} G\left(k,0\right) = \frac{k}{\pi}, \qquad \lim_{k\to\infty} G\left(k,0\right) = \frac{1}{2}\cdot$$

The long-wavelength limit of the dynamic local field factor will be calculated explicitly.

For finite frequency, $\nu \geq k + k^2/2$, only the long-wavelength behavior of $\mathrm{Re}\left\{Q_0\left(k,\nu\right)\right\}$ and $\mathrm{Re}\left\{I_G\left(k,\nu\right)\right\}$ needs to be calculated to obtain the long wavelength limit of $G\left(k,\nu\right)$. For $\mathrm{Re}\left\{Q_0\left(k,\nu\right)\right\}$, it is easily shown that

$$\lim_{k\to 0,\nu>k^2/2+k} \mathrm{Re}\left\{Q_0\left(k,\nu\right)\right\} = -\,r_s\frac{\sqrt{2}}{2\nu^2}k\left(1+\frac{3}{4}\frac{k^2}{\nu^2}\right)+O\left(k^4\right). \tag{B.1}$$

The calculation of the long-wavelength limit of $\mathrm{Re}\left\{I_G\left(k,\nu\right)\right\}$ is more involved. For $k \to 0$ and finite frequency, the frequency denominators in expression (3) can be expanded. Introducing Cartesian coordinates with the $x-$ and $\xi - axis$ chosen along $\mathbf{k}$, one finds

$$\lim_{k\to 0}\left(\frac{1}{\left(\nu-xk\right)^2}\frac{1}{\left(\nu-\xi k\right)}\right) = \frac{1}{\nu^3}\left(1+2\frac{x}{\nu}k\right)\left(1+\frac{\xi}{\nu}k\right). \tag{B.2}$$

To first order in k, the real part $\mathrm{Re}\left\{I_G\left(k,\nu\right)\right\}$ becomes

$$\lim_{k\to 0,\nu>k^2/2+k} \mathrm{Re}\left\{I_G\left(k,\nu\right)\right\} = \frac{1}{\nu^3}k\int d^2r\int d^2r'\frac{\left(-x+\xi\right)\left(1+\frac{k}{\nu}\left(2x+\xi\right)\right)}{|\mathbf{r}-\mathbf{r}'|} \times\left(\mathcal{N}\left(\mathbf{r}+\frac{\mathbf{k}}{2}\right)-\mathcal{N}\left(\mathbf{r}-\frac{\mathbf{k}}{2}\right)\right) \times\left(\mathcal{N}\left(\mathbf{r}'+\frac{\mathbf{k}}{2}\right)-\mathcal{N}\left(\mathbf{r}'-\frac{\mathbf{k}}{2}\right)\right). \tag{B.3}$$

If k tends to zero, the difference of cut-off functions $\mathcal{N}\left(\mathbf{r}\right)$ can be written as

$$\lim_{k\to 0}\left(\mathcal{N}\left(\mathbf{r}+\frac{\mathbf{k}}{2}\right)-\mathcal{N}\left(\mathbf{r}-\frac{\mathbf{k}}{2}\right)\right) = -\left(\mathbf{r}\cdot\mathbf{k}\right)\delta\left(|\mathbf{r}|-1\right), \tag{B.4}$$

leading to

$$\lim_{k\to 0,\nu>k^2/2+k} \mathrm{Re}\left\{I_G\left(k,\nu\right)\right\} = \frac{1}{\nu^3}k^3\int d^2r\int d^2r'\frac{\delta\left(|\mathbf{r}|-1\right)\delta\left(|\mathbf{r}'|-1\right)}{|\mathbf{r}-\mathbf{r}'|} \times\left(1+\frac{k}{\nu}\left(2x+\xi\right)\right)x\xi\left(-x+\xi\right). \tag{B.5}$$

Symmetry considerations show that the lowest order term in k now vanishes. One is left with

$$\lim_{k\to 0,\nu>k^2/2+k} \mathrm{Re}\left\{I_G\left(k,\nu\right)\right\} = \frac{k^4}{\nu^4}\int d^2r\int d^2r' x\xi\left(\xi+2x\right)\left(-x+\xi\right) \times\frac{\delta\left(|\mathbf{r}|-1\right)\delta\left(|\mathbf{r}'|-1\right)}{|\mathbf{r}-\mathbf{r}'|}\cdot \tag{B.6}$$

In polar coordinates (ρ,ϕ) and (σ,θ), the integrations over the radial variables are performed instantly

$$\lim_{k\to 0,\nu>k^2/2+k} \mathrm{Re}\left\{I_G\left(k,\nu\right)\right\} = \frac{k^4}{2\nu^4}\int_{-\pi}^{\pi}d\phi\int_{-\pi}^{\pi}d\theta\cos\phi\cos\theta \times\frac{\left(\cos\theta+2\cos\phi\right)\left(\cos\theta-\cos\phi\right)}{\left|\sin\left(\frac{\phi-\theta}{2}\right)\right|}\cdot \tag{B.7}$$

The sinus function in the denominator can then be expanded as

$$\sin\left(\frac{\phi-\theta}{2}\right) = \sqrt{\frac{1+\cos\theta}{2}}\sqrt{\frac{1+\cos\phi}{2}}\left(\tan\frac{1}{2}\phi-\tan\frac{1}{2}\theta\right). \tag{B.8}$$

Introducing the new integration variables $s = \tan\left(\phi/2\right)$ and $t = \tan\left(\theta/2\right)$, transforms the integral into

see equation (B.9) above

where the use of general symmetry properties of the integrand allowed us to reduce the integration interval. The remaining integrations are elementary but a bit lengthy. Eventually, one is left with

$$\lim_{k\to 0,\nu>k^2/2+k} \mathrm{Re}\left\{I_G\left(k,\nu\right)\right\} = \frac{5}{3}\frac{k^4}{\nu^4}\pi. \tag{B.10}$$

Combining the expressions (2), (B.1) and (B.10), yields

$$\lim_{k\to 0,\nu>k^2/2+k} \mathrm{Re}\left\{G\left(k,\nu\right)\right\} = \frac{5}{6\pi}k, \tag{B.11}$$

to lowest order in k.

References

1. M. Jonson, J. Phys. C **9**, 3055 (1976)
2. J. Hubbard, Proc. Roy. Soc. A **243**, 336 (1957)
3. K.S. Singwi, M.P. Tosi, R.H. Land, A. Sjölander, Phys. Rev. **176**, 589 (1968)
4. B. Davoudi, M. Polini, G.F. Giuliani, M.P. Tosi, Phys. Rev. B **64,** 153101 (2001)
5. M.W.C. Dharma-wardana, F. Perrot, `xxx.lanl.gov/abs/cond-mat/0211127`
6. A. Kugler, J. Stat. Phys. **8**, 107 (1973); *ibid.* **12**, 35 (1975)
7. J.C. Kimball, Phys. Rev. A **7**, 1648 (1973); J.C. Kimball, Phys. Rev. B **14**, 2371 (1976)
8. A. Czachor, A. Holas, S.R. Sharma, K.S. Singwi, Phys. Rev. B **25**, 2144 (1982)
9. K. Takayanagi, E. Lipparini, Phys. Rev. B **52**, 1738 (1995); *ibid.* **54**, 8122 (1996); F. Pederiva, E. Lipparini, K. Takayanagi, Europhys. Lett. **40**, 607 (1997)
10. H.-J. Schulze, P.Schuck, N. Van Giai, Phys. Rev. B **61**, 8026 (2000)
11. F. Brosens, L.F. Lemmens, J.T. Devreese, Phys. Stat. Sol. (b) **74**, 45 (1976)
12. J.T. Devreese, F. Brosens, L.F. Lemmens, Phys. Rev. B **21**, 1349 (1980); F. Brosens, J.T. Devreese, L.F. Lemmens, *ibid.* **21**, 1363 (1980)
13. K.J. Hameeuw, F. Brosens, J.T. Devreese, Solid State Commun. **126**, 695 (2003)
14. A.K. Rajagopal, Phys. Rev. **142**, 152 (1965)
15. G. Niklasson, Phys. Rev. B **10**, 3052 (1974)
16. P.E. Batson, C.H. Chen, J. Silcox, Phys. Rev. Lett. **37**, 937 (1976)
17. B.C. Larson, J.Z. Tischler, E.D. Isaacs, P. Zschack, A. Fleszar, A.G. Eguiluz, Phys. Rev. Lett. **77**, 1346 (1996)
18. J.Z. Tischler, B.C. Larson, P. Zschack, A. Fleszar A.G. Eguiluz, Phys. Stat. Sol. (b) **237**, 280 (2003)
19. F. Stern, Phys. Rev. Lett. **18**, 546 (1967)
20. F. Brosens, L.F. Lemmens, J. Ruvalds, J.T. Devreese, Phys. Rev. B **39,** 11139 (1989)
21. F. Perrot, M.W.C. Dharma-wardana, PRL **87**, 206404 (2002)
22. N. Iwamoto, Phys. Rev. A **30**, 3289 (1984)
23. A.K. Rajagopal, J.C. Kimball, Phys. Rev. B **15**, 2819 (1977)
24. F. Brosens, L.F. Lemmens, J.T. Devreese, Phys. Stat. Sol. (a) **59**, 447 (1980)